Journal of Photochemistry and Photobiology B: Biology 107 (2012) 20–26

Contents lists available at SciVerse ScienceDirect

Journal of Photochemistry and Photobiology B: Biology

journal homepage: www.elsevier.com/locate/jphotobiol

Interaction of 5-Fluorouracil and its derivatives with bovine serum albumin

K. Abdi [a], Sh. Nafisi [b,c,*], F. Manouchehri [b], M. Bonsaii [b], A. Khalaj [a]

[a] Department of Medicinal Chemistry and Radiopharmacy, Faculty of Pharmacy, Tehran University of Medical Sciences, Tehran, Iran
[b] Department of Chemistry, Islamic Azad University, Central Tehran Branch (IAUCTB), Tehran, Iran
[c] Research Institute for Islamic and Complementary Medicine, Tehran University of Medical Sciences, Tehran, Iran

ARTICLE INFO

Article history:
Received 13 September 2011
Received in revised form 14 November 2011
Accepted 17 November 2011
Available online 23 November 2011

Keywords:
Bovine serum albumin
5-Fluorouracil
FUPAE
FUPAP
FTIR
UV–Vis

ABSTRACT

Fluorouracil (5-FU) and its derivatives are the most commonly used drugs to treat many types of cancer. Two dual functional agents, FUPAE and FUPAP, derived from 5-Fluorouracil (5-FU) have shown radiosensitizing activity but unlike their components were not cytotoxic. This study was designed to examine the interaction of BSA with 5-Fluorouracil (5-FU) and two of its derivatives; FUPAE and FUPAP at physiological conditions, using a constant protein concentration and various drug contents. FTIR, UV–Vis spectroscopic methods as well as molecular modelling were used to determine the drugs binding mode, the binding constants and the effects of drug complexation on BSA stability and conformation. Structural analysis showed that 5-Fluorouracil, FUPAE and FUPAP bind BSA via polypeptide polar groups with overall binding constants of $K_{5\text{-FU–BSA}} = 3.02(\pm0.09) \times 10^3$, $K_{\text{FUPAE–BSA}} = 1.08(\pm0.04) \times 10^4$, $K_{\text{FUPAP–BSA}} = 1.21(\pm0.06) \times 10^4\ M^{-1}$. BSA conformation was altered by a major reduction of α-helix from 69% (free BSA) to 34% with 5-FU, 40% with FUPAE, 38% with FUPAP. These results suggest that serum albumins might act as carrier proteins for FUPAE and FUPAP in delivering them to target tissues.

1. Introduction

5-FU is a chemotherapeutic agent which has been used mainly for colorectal and pancreatic and aggressive forms of breast cancers. It has also been used as an anti-scarring agent in ophthalmic surgery and topically for treatment of actinic kurtosis and some types of skin cancers [1–5]. 5-FU (Scheme 1A) is a pyrimidine analogue drug which shows radiosensitizing activity. On the basis of the radiosensitizing activities of aromatic nitro compounds [6–9], the synthesis of 2,4-dinitrophenylamine tethered to 5-fluoracil through 2 and 3 carbon atoms has been reported; [3-(2-(2,4-dinitrophenylamino)ethyl)-5-fluoropyrimidine-2,4(1H,3H)-dione] (FUPAE) and [3-(3-(2,4-dinitrophenylamino)propyl)-5-fluoropyrimidine-2,4(1H,3H)-dione] (FUPAP) [10] (Scheme 1A). The synthesis reaction is shown in Scheme 1B. Originally it was anticipated that these compounds like 2,4-dinitrophenylamine mustards and dinitroaziridin have radiosensitizing activity as well as aerobic cytotoxicity due to the parent nitro compounds or bio-activation by NADPH: quinooxidoreductase (DT diphrace) as an oxygen-insensitive reductase [11–14]. However, the results showed that these compounds unlike their components were not cytotoxic but increased the sensitivity of the normal oxygenated cells to radiation [10].

One of the important properties of a drug is the degree of its protein binding which affects the drug effective solubility, biodistribution, half life in the body and interaction with other endogenous or exogenous compounds. The proteins commonly involved with drug delivery are serum albumin, lipoproteins, and al-glycoprotein. Serum albumin is the most abundant protein present in the circulatory system of a wide variety of organisms and is the major macromolecule contributing to the osmotic blood pressure [15]. The most important property of this group of proteins is that they serve as transporters for a variety of compounds. BSA (Scheme 2) has been one of the most extensively studied of this group of proteins, particularly because of its structural homology with human serum albumin (HSA). The BSA molecule is made up of three homologous domains (I, II, III) that are divided into nine loops (L1–L9) by 17 disulphide bonds. Each domain in turn is the product of two sub-domains (IA, IB, etc.). X-ray crystallographic data [16] shows that the albumin structure is predominantly α-helical and the remaining polypeptide chain occurs in turns and extended or flexible regions between sub-domains without β-sheets. BSA has two tryptophan residues, Trp-134 in the first domain and Trp-212 in the second domains that possess intrinsic fluorescence [17]. Trp-212 is located within a hydrophobic binding pocket of the protein and Trp-134 is located on the surface of the molecule [18]. Plasma protein binding of drugs assumes great importance since it influences their pharmacokinetic and pharmacodynamic properties, and may also cause interference with the binding of other endogenous and/or

* Corresponding author at: Department of Chemistry, Islamic Azad University, Central Tehran Branch (IAUCTB), Tehran, Iran. Tel./fax: +1 98 21 22426554.
E-mail address: drshnafisi@gmail.com (Sh. Nafisi).

1011-1344/$ - see front matter © 2011 Elsevier B.V. All rights reserved.
doi:10.1016/j.jphotobiol.2011.11.004

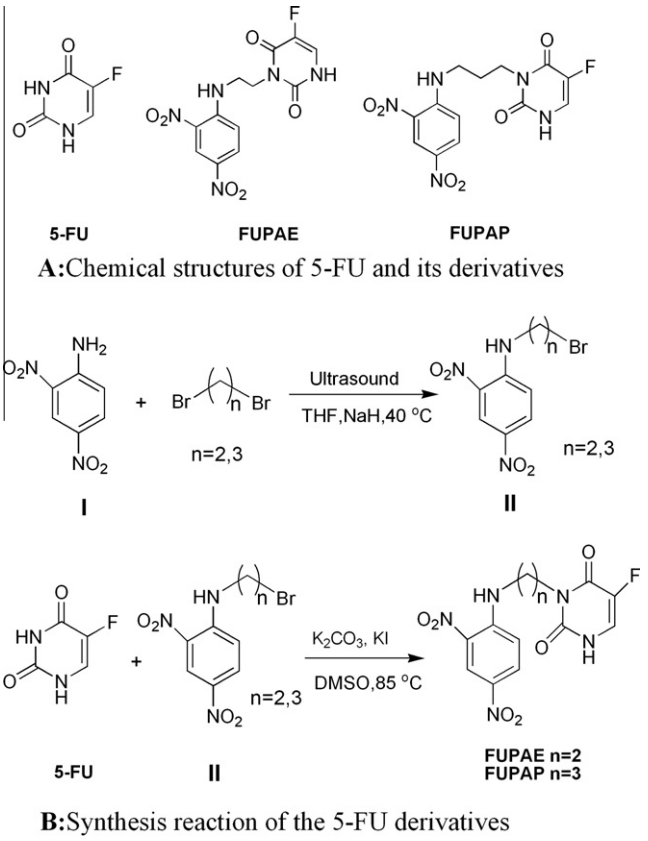

Scheme 1. (A) Chemical structures of 5-FU and its derivatives. (B) Synthesis reaction of the 5-FU derivatives; FUPAE, FUPAP.

exogenous ligands as a result of overlap of binding sites and/or conformational changes [19,20].

In this report, spectroscopic analyses and molecular modelling of the interaction of 5-FU, FUPAE and FUPAP (Scheme 1A) with BSA has been reported in aqueous solution under physiological conditions and using constant concentration of protein and different concentrations of ligands. Structural information on binding modes of 5-FU, FUPAE and FUPAP and the effects of ligand–protein complexation on the stability and conformation of BSA are also reported.

2. Materials and methods

2.1. Materials

Bovine serum albumin fraction V (free fatty acid) was purchased from Sigma Chemical Co. 5-FU was obtained from Merck Chemical Co. and used as supplied. Other chemicals were of reagent grade and used without further purification. FUPAE and FUPAP were synthesized according to the previous literature [10]. Briefly, compound II was prepared by ultrasound promoted reaction of 2,4-dinitrophenylamine (compound I) with related dibromoalkane. Finally FUPAE and FUPAP were synthesized by the reaction of 5-Fluorouracil (5-FU) with related compound II (Scheme 1B). The synthesized compounds were purified by column chromatography and then crystallized. The purity of the synthesized compounds was determined by TLC and NMR (Purity > 98%).

2.2. Preparation of stock solutions

Bovine serum albumin (40 mg/mL or 0.5 mM) was dissolved in aqueous solution containing phosphate buffer (pH 7.2). The protein

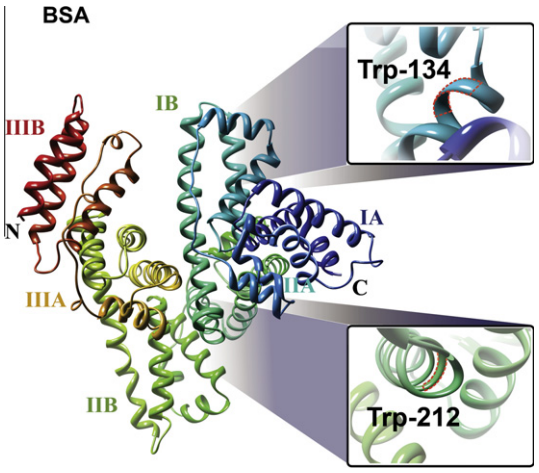

Scheme 2. Bovine serum albumin (each sub-domain is marked in a different color) with tryptophan residues shown in close up view with red color dash-line. (For interpretation of the references to colour in this figure legend, the reader is referred to the web version of this article.)

concentration was determined spectrophotometrically using an extinction coefficient of 36,500 M^{-1} cm^{-1} at 280 nm [21]. Solutions of 5-FU, FUPAE and FUPAP (1 mM) were first prepared in phosphate buffer/ethanol 50% and then diluted by serial dilution to 0.500, 0.125, 0.062, 0.015 mM in the same phosphate buffer. After addition of an equal volume of 5-FU, FUPAE, FUPAP to protein solution, the final ethanol concentration was reduced to 25%. The presence of 25% of ethanol induces no major BSA structural changes according to the literature report [22].

2.3. FTIR spectroscopic measurements

Infrared spectra were recorded on a Nicolet FTIR spectrometer (Magna-IR 550) equipped with a liquid-nitrogen-cooled HgCdTe (MCT) detector and a KBr beam splitter, using AgBr windows. Solutions of 5-FU, FUPAE and FUPAP were added dropwise to the BSA solution with constant stirring to ensure the formation of homogeneous solution and to have ligands concentrations of 0.015, 0.062, 0.125, 0.5 and 1 mM with a final protein concentration of 0.25 mM (20 mg/mL). The concentrations of the ligands in the complex mixtures were 7.5×10^3, 0.031, 0.0.062, 0.25 and 0.5 Mm. Spectra were collected after 2 h of incubation of BSA with drug solution at room temperature, using hydrated films. Interferograms were accumulated over the spectral range 4000–600 cm^{-1} with a nominal resolution of 2 cm^{-1} and 100 scans. The difference spectra [(protein solution + pyrimidine analogues solutions) – (protein solution)] were generated using the water combination mode around 2300 cm^{-1}, as the standard [23]. When producing difference spectra, this band was adjusted to the baseline level, in order to normalize difference spectra.

2.4. Analysis of protein conformation

Analysis of the secondary structure of BSA and complexes was carried out according to the previously reported method [24]. The protein secondary structure is determined from the shape of the amide I band, located around 1660–1650 cm^{-1}. The FTIR spectra were smoothed, and their baselines were corrected automatically using Grams AI software. Thus, the root-mean square (rms) noise of every spectrum was calculated. By means of the second derivative in the spectral region 1700–1600 cm^{-1}, the major peaks for BSA and the complexes were resolved. The above spectral region was deconvoluted by the curve-fitting method with the Levenberg–Marquadt algorithm and the peaks corresponding to α-helix (1658–

1651 cm^{-1}), β-sheet (1640–1610 cm^{-1}), turn (1670–1665 cm^{-1}), random coil (1648–1641 cm^{-1}), and β-antiparallel (1692–1680 cm^{-1}) were adjusted and the area measured with the Gaussian function. The area of all component bands assigned to a given conformation were then summed up and divided by the total area [25,26]. The curve-fitting analysis was performed using the GRAMS/AI Version 7.01 software of the Galactic Industries Corporation.

2.5. Absorption spectroscopy

The absorption spectra were recorded on a Cecil BioAquarius CE 7250 double beam spectrophotometer, using a slit of 5 nm and a scan speed of 250 nm min^{-1}. Quartz cuvettes of 1 cm were used. The UV absorption of BSA in the presence and absence of 5-FU, FUPAE, FUPAP solutions were measured at pH 7.2 by keeping the concentration of BSA constant (0.025 mM), while varying the concentration of the drug (1 μM–1 mM), in the range of 250–550 nm.

The binding constants of the drugs–BSA complexes were calculated as reported [27]. It is assumed that the interaction between the ligand L and the substrate S is 1:1; for this reason, a single complex SL (1:1) is formed. It was also assumed that the sites (and all the binding sites) are independent and finally the Beer's law is followed by all species. A wavelength is selected at which the molar absorptivities, ε_S (molar absorptivity of the substrate) and ε_{11} (molar absorptivity of the complex) are different. Then at total concentration *St* of the substrate, in the absence of ligand and the light path length is $b = 1$ cm, the solution absorbance is:

$$A_0 = \varepsilon_S b S_t \tag{1}$$

In the presence of ligand at total concentration *Lt*, the absorbance of a solution containing the same total substrate concentration is:

$$A_L = \varepsilon_S b[S] + \varepsilon_L b[L] + \varepsilon_{11} b[SL] \tag{2}$$

where [*S*] is the concentration of the uncomplexed substrate, [*L*] is the concentration of the uncomplexed ligand and [*SL*] is the concentration of the complex) which, combined with the mass balance on *S* and *L*, gives:

$$A_L = \varepsilon_S b S_t + \varepsilon_L b L_t + \Delta\varepsilon_{11} b[SL] \tag{3}$$

where $\Delta\varepsilon_{11} = \varepsilon_{11} - \varepsilon_S - \varepsilon_L$ (ε_L molar absorptivity of the ligand). By measuring the solution absorbance against a reference containing ligand at the same total concentration *Lt*, the measured absorbance becomes:

$$A = \varepsilon_S b S_t + \Delta\varepsilon_{11} b[SL] \tag{4}$$

Combining Eq. (4) with the stability constant definition $K_{11} = [SL]/[S][L]$, gives:

$$\Delta A = K_{11}\Delta\varepsilon_{11} b[S][L] \tag{5}$$

where $\Delta A = A - A_0$. From the mass balance expression $S_t = [S] + [SL]$, we get $[S] = S_t/(1 + K_{11}[L])$, which is Eq. (5), giving Eq. (6) at the relationship between the observed absorbance change per centimeter and the system variables and parameters.

$$\frac{\Delta A}{b} = \frac{S_t K_{11}\Delta\varepsilon_{11}[L]}{1 + K_{11}[L]} \tag{6}$$

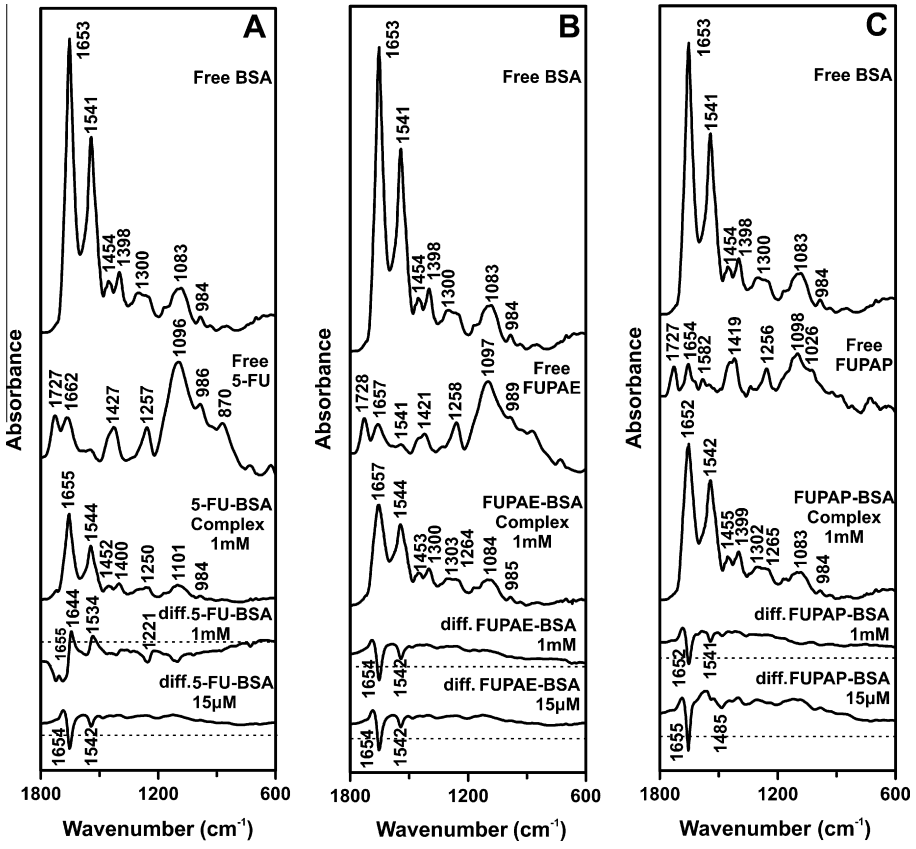

Fig. 1. FTIR spectra in the region of 1800–600 cm^{-1} of hydrated films (pH 7.2) for free BSA (0.5 mM), (A) free 5-FU (1 mM), (B), free FUPAE (1 mM), (C) free FUPAP (1 mM) and their BSA complexes with difference spectra (diff.) (bottom two curves) obtained at different drug concentrations (indicated on the figure).

Eq. (6) is the binding isotherm, which shows the hyperbolic dependence on free ligand concentration. The double-reciprocal form of plotting the rectangular hyperbola, is based on the $\frac{1}{y} = \frac{f}{d} \cdot \frac{1}{x} + \frac{e}{d}$, linearization of Eq. (6) according to the following equation:

$$\frac{b}{\Delta A} = \frac{1}{S_t K_{11} \Delta\varepsilon_{11}[L]} + \frac{1}{S_t \Delta\varepsilon_{11}} \quad (7)$$

Thus the double reciprocal plot of $1/\Delta A$ versus $1/[L]$ is linear and the binding constant can be estimated from the following equation:

$$K_{11} = \frac{\text{intercept}}{\text{slope}} \quad (8)$$

2.6. Molecular modelling and docking

2.6.1. Model of bovine serum albumin

Structure of BSA was predicted by automated homology modelling using SWISS-MODEL Workspace [28,29]. The structure of free HSA (PDB id: 1AO6, chain A) obtained by X-ray crystallography [30] was used as a template. BSA and HSA proteins share 78.1% of sequence identity, which is sufficient to obtain reliable sequence alignment [17,31]. Images of the structures were generated using UCSF Chimera 1.5.3 (Web address: http://www.cgl.ucsf.edu/chimera) (Scheme 2). Root Mean Standard Deviation (RMSD) between model and template proteins was 0.20 Å for positions of backbone atoms, as calculated with DeepView/Swiss-PdbViewer 4.0.1. By using the structure and model assessment tools of SWISS-MODEL workspace, it was found that the quality of the predicted BSA structure is similar to the structure of the free HSA which was used as a template.

Table 1
Secondary structure analysis (infrared spectra) from the free BSA and its complexes in hydrated film at pH 7.2.

Complex (ligand concentration (mM))	α-Helix (±3%)	β-Anti (±1%)	β-Sheet (±2%)	Turn (±2%)	Random (±1%)
Free BSA	69	3	12	14	2
5-FU–BSA (1 mM)	34	3	9	40	3
5-FU–BSA (15 μM)	40	5	16	31	2
FUPAE–BSA (1 mM)	40	6	15	31	8
FUPAE–BSA (15 μM)	39	4	16	34	7
FUPAP–BSA (1 mM)	38	5	13	37	6
FUPAP–BSA (15 μM)	39	3	12	43	3

2.6.2. Molecular docking

To determine the preferred binding sites on BSA, the docking studies were performed by AutoDock 4.2.3 software (http://autodock.scripps.edu).

By using genetics algorithm (GA) for the local search, the so-called pseudo-Solis and Wets algorithm was applied using a maximum of 300 iterations per local search [32].

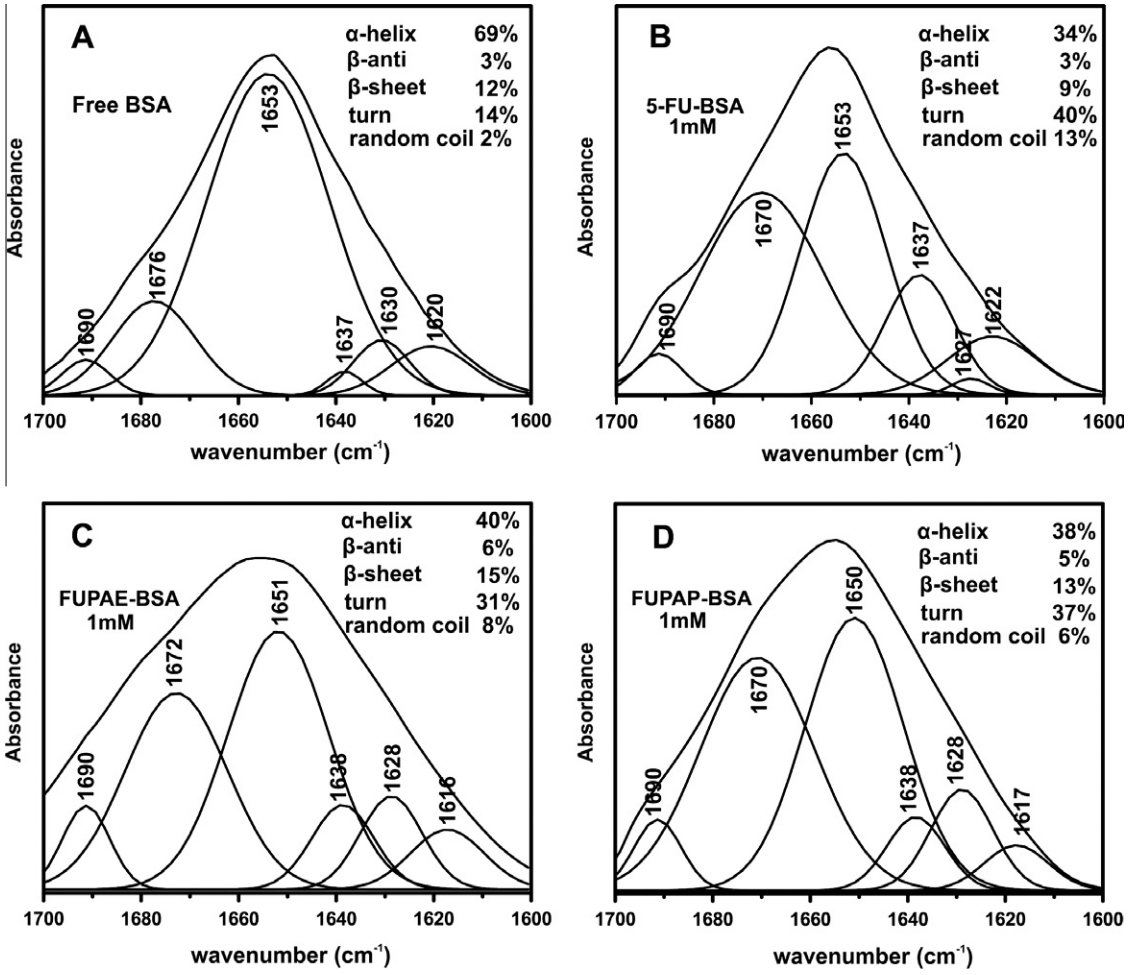

Fig. 2. Second derivative resolution enhancement and curve-fitted amide-I region (1700–1600 cm^{-1}) for free BSA and its drug adducts in aqueous solution with 1 mM drug for 5-FU, FUPAE and FUPAP concentrations at pH 7.2.

In AutoDock, the overall docking energy of a given ligand molecule in its active site is expressed as follows:

$$\Delta G = \Delta G_{vdW} \sum_{i,j} \left(\frac{A_{ij}}{r_{ij}^{12}} - \frac{B_{ij}}{r_{ij}^{6}} \right) + \Delta G_{hbond} \sum_{i,j} \left(\frac{C_{ij}}{r_{ij}^{12}} - \frac{D_{ij}}{r_{ij}^{10}} + E_{hbond} \right) + \Delta G_{elec} \sum_{i,j} \frac{q_i - q_j}{\varepsilon(r_{ij}) r_{ij}} + \Delta G_{tor} N_{tor} + \Delta G_{sol} \sum_{i \subset j} S_i V_j e^{\left(-r_{ij}^2/2\sigma^2\right)} \quad (9)$$

where ΔG_{vdW}, ΔG_{hbond}, ΔG_{elec}, ΔG_{tor}, and ΔG_{sol} are free energy coefficients of van der Waals, hydrogen bond, electrostatic interactions, torsional term, and desolvation energy of oligonucleotide–ligand complex, respectively. r_{ij}, A_{ij}, B_{ij}, C_{ij}, and D_{ij} represent the interatomic distance, the depths of energy well, and the equilibrium separations between the two atoms, respectively. The first three terms are in vacuo force field energies for intermolecular interactions. The fourth term accounts for the internal steric energy of the ligand molecule.

The energies used and reported by AutoDock should be distinguished since there are docked energies, which include the intermolecular and intramolecular interaction energies, and are used during dockings to predict free energies; including the intermolecular energy and torsional free energy, and are only reported at the end of a docking [33].

The relationship between binding constant, $K_{binding}$ and the binding free energy change of binding, $\Delta G_{binding}$ is as follows:

$$\Delta G_{binding} = -RT \ln K_{binding} \quad (10)$$

where R is the gas constant, 1.987 cal K^{-1} mol^{-1}, and T is the absolute temperature, 298.15 K.

AutoDock Tools1.5.4 (ADT) (Web address: http://mgltools.scripps.edu) and UCSF Chimera 1.5.3 were used for the analysis of display docking results.

3. Results and discussion

3.1. FTIR spectra of 5-FU, FUPAE and FUPAP–BSA complexes

The 5-FU, FUPAE, FUPAP–BSA interaction was characterized by infrared spectroscopy and its derivative methods. Since there was no major spectral shifting for the protein amide I band at 1653 cm^{-1} (mainly C=O stretch) and amide II band at 1541 cm^{-1} (C–N stretching coupled with N–H bending modes) [24,34] upon pyrimidine analogues interaction, the difference spectra [(protein

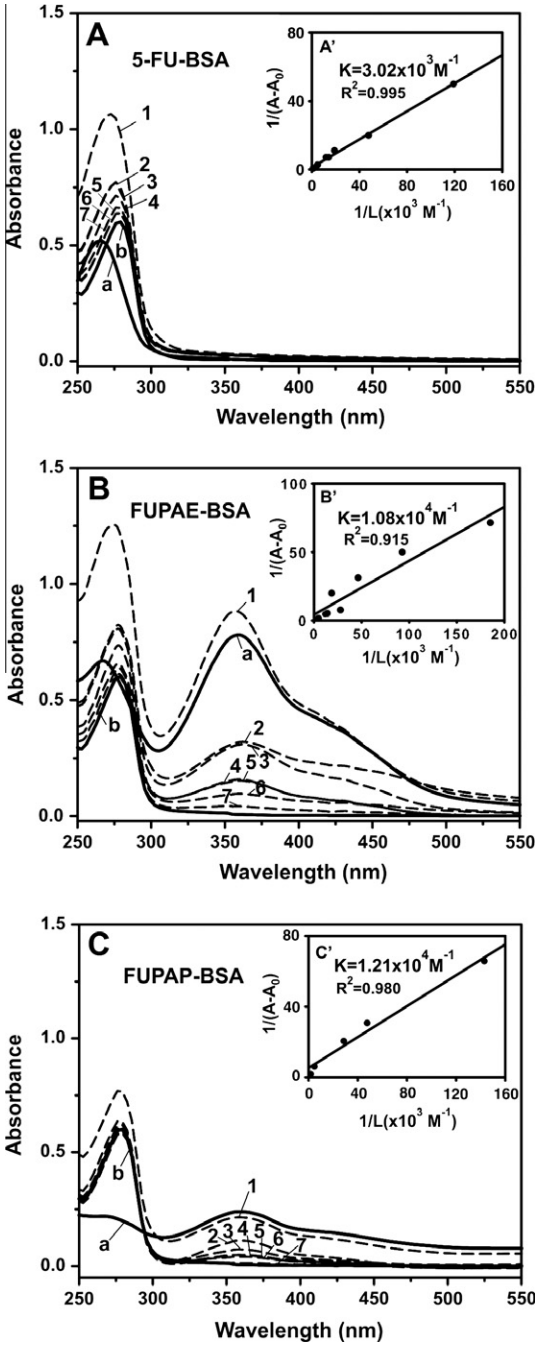

Fig. 3. UV–Vis results of free BSA and its drug complexes in aqueous solution spectra of (a) free drug (0.21 mM); (b) free BSA (0.025 mM); (1–7) drug–BSA complexes; 1 (0.21 mM), 2 (0.084 mM), 3 (0.071 mM), 4 (0.054 mM), 5 (0.035 mM), 6 (0.021 mM) and 7 (0.01 mM). Plot of $1/(A - A_0)$ versus (1/drug concentration), where A_0 is the initial absorbance of BSA (279 nm) and A is the recorded absorbance at different 5-FU, FUPAE and FUPAP concentrations (0.21–0.01 mM) with constant BSA concentration of 0.025 mM at pH 7.2.

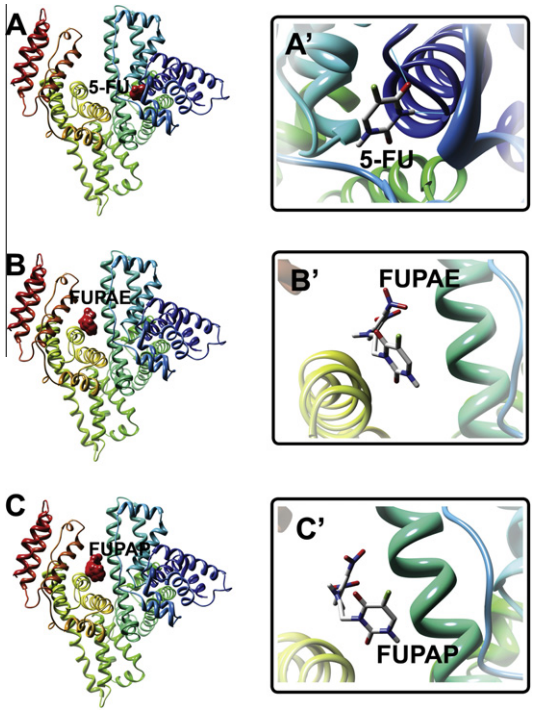

Fig. 4. Docking structure between ligands and BSA. (A) Ribbon representation of BSA complexes with 5-FU. 5-FU was shown in red surface (display side). (A′) Close up view of BSA complexes with 5-FU. Outcome is represented by stick style. Hydrogen bond between BSA and 5-FU are represented by Pale Turquoise line. (B) and (C) Ribbon representations of BSA complexes with FUPAE and FUPAP. (For interpretation of the references to colour in this figure legend, the reader is referred to the web version of this article.)

Table 2
Amino acid residues involved in drug–BSA interaction with the free binding energy for the best-selected docking positions from docking study and experimental data from UV–Vis spectroscopy.

Complex	Residues involved in the interaction	$\Delta G_{binding}$ (kcal/mol)	
		Calculated	Experimental
BSA–5-FU	Try30, Leu31, Gln32, Gln33, Met87, Lis106, Asp107	−4.39	−4.75
BSA–FUPAE	Arg186, Lys 190, Pro421, Arg428, Lys432	−5.3	−5.5
BSA–FUPAP	Asn109, Arg186, Lys190, Pro421, Arg428, Lys432	−5.53	−5.6

solution + pyrimidine analogues solutions) − (protein solution)] were obtained, in order to monitor the intensity variations of these vibrations and the results are shown in Fig. 1. Similarly, the infrared self deconvolution with second derivative resolution enhancement and curve-fitting procedures [24] were used to determine the protein secondary structures in the presence of pyrimidine analogues–BSA complexes (Fig. 2 and Table 1).

At different pyrimidine analogues concentrations (15 μM, 1 mM), decrease in intensity of the amide I band at 1653 cm^{-1} (BSA) was observed with features at 1654 cm^{-1} (5-FU–BSA, FUPAE–BSA) and at about 1652 cm^{-1} (FUPAP–BSA) for 15 μM and at 1655 cm^{-1} (5-FU–BSA), 1654 cm^{-1} (FUPAE–BSA) and 1652 (FUPAP–BSA) for 1 mM.

In the difference spectra of pyrimidine analogues–BSA complexes (Fig. 1, diff, 15 μM, 1 mM), negative features are due to the reduction of intensity due to loss of protein structure (Fig. 1) of the amide I band and suggests a major reduction of protein α-helical structure at different pyrimidine analogues concentrations. Similar infrared spectral changes were observed for the protein amide I band in several ligand–protein complexes, where major protein conformational changes occurred [35,36].

A quantitative analysis of the protein secondary structure for the free BSA and its pyrimidine analogues adducts in hydrated films has been carried out, and the results are shown in Fig. 2 and Table 1. The free protein was 69% α-helix (1653 cm^{-1}), 12% β-sheet (1620 cm^{-1}), 14% turn structure (1676 cm^{-1}), 3% β-anti-parallel (1690 cm^{-1}), and 2% random coil (1637 cm^{-1}) (Fig. 2 and Table 1). The results are consistent with the spectroscopic studies of bovine serum albumin previously reported [37,38]. Upon pyrimidine analogues interaction, a major decrease of α-helix from 69% (free BSA) to 34% (5-FU–BSA,1 mM), 40% (FUPAE–BSA, 1 mM), and 38% (FUPAP–BSA, 1 mM) with changes in β-sheet from 12% (free BSA) to 9% (5-FU–BSA,1 mM), and 15% (FUPAE–BSA, 1 mM) and 13% FUPAP–BSA were observed (Fig. 2 and Table 1). A similar increase was also observed for the turn structure from 14% (free BSA) to 40% (5-FU–BSA, 1 mM), 31% (FUPAE–BSA, 1 mM), and 37% (FUPAP–BSA, 1 mM) (Fig. 2 and Table 1). These results are consistent with the decrease in intensity of the protein amide I band discussed above. The decrease in α-helix structure and increase in β-sheet and turn structures is indicative of protein destabilization upon 5-FU and its derivatives interaction.

3.2. UV spectra and stability of pyrimidine analogues–BSA complexes

An increase in the 5-FU, FUPAE, FUPAP concentrations resulted in an increase in UV light absorption and shifting of BSA band at 279–274 nm that can be related to complex formation (Fig. 3). The binding constants of the complexes were also determined using UV–Visible spectroscopic method (described in Materials and methods). The double reciprocal plot of $1/(A - A_0)$ versus 1/(ligand concentration) is linear and the binding constant (K) can be estimated from the ratio of the intercept to the slope (Fig. 3). A_0 is the initial absorbance of the free BSA at 280 nm and A is the recorded absorbance at different drug concentrations (Fig. 3). One binding site was observed for each ligand–protein complex with the overall binding constants of $K_{5\text{-FU–BSA}} = 3.02(\pm0.09) \times 10^3$, $K_{\text{FUPAE–BSA}} = 1.08(\pm0.04) \times 10^4$, $K_{\text{FUPAP–BSA}} = 1.21(\pm0.06) \times 10^4$ M^{-1} (Fig. 3). The order of binding is FUPAP–BSA > FUPAE–BSA > 5-FU–BSA. Similar binding constants were observed for tamoxifen and its metabolites protein complexes [39]. The association constants calculated for the tested compounds–BSA complexes suggest a low affinity for complex formation, compared to strong ligand–protein complexes, with binding constants ranging from 10^6 M^{-1} to 10^8 M^{-1} [39–41].

3.3. Docking

5-FU, FUPAE, and FUPAP molecules were docked to BSA to determine the preferred binding sites on the protein and the results are shown in Fig. 4 and Table 2. Data drived from docking of the tested compounds to BSA, showed different moods of interactions. The free energy of the binding of the most compatible structure with FTIR and UV results are shown in Table 2. The models show that 5-FU is surrounded by Try30, Leu31, Gln32, Gln33, Met87, Lis106, and Asp107 (subdomains of IA and IB) with a binding energy of −4.39 kcal/mol. The 5-FU–BSA docking results indicated the presence of hydrogen bond between O4 of 5-FU and nitrogen of the amine in Gln33 of BSA and H3 of 5-FU and oxygen of amide, in Tyr30, which stabilizes 5-FU–BSA complexes (Fig. 4A′). The results showed different mechanisms of the interaction of 5-FU and its derivatives with BSA. FUPAE and FUPAP mainly interact with the positively charged amino acids and the binding sites are located at the surface between subdomains IB and IIIA (Fig. 4B′ and C′). The orders of the stability of drug–BSA complexes obtained from docking study is consistent with those of the spectroscopic results showing FUPAP–BSA > FUPAE–BSA > 5-FU–BSA (Fig. 3 and Table 2).

4. Conclusion

Results of this study present important quantitative data on the binding affinity of 5-FU and its derivatives to bovine serum albumin, a drug carrier protein. It was also showed distinct differences in the mode of protein binding between the parent drug and its derivatives. The interaction of 5-FU and its derivatives with BSA can be used to gain insight into the mechanism of action of 5-FU in cancer therapy and synthesizing new drugs. Based on our spectroscopic data, pyrimidine analogues binding to BSA occurs and causes a partial protein destabilization. The affinity of pyrimidine analogues–protein complexation is FUPAP > FUPAE > 5-FU with the binding constants of $K_{5\text{-FU–BSA}} = 3.02(\pm0.09) \times 10^3$, $K_{\text{FUPAE–BSA}} = 1.08(\pm0.04) \times 10^4$, $K_{\text{FUPAP–BSA}} = 1.21 \pm (0.06) \times 10^4$ M^{-1}. The pyrimidine analogues–BSA binding site is mainly in the vicinity of the non-acidic amino acids and positively charged amino acid located in the protein domains I and III in two 5-FU derivatives. It is important to note here that the low affinity binding is consistent with the role of serum proteins as carrier molecules for the delivery of the parent drug and its derivatives to target tissues.

Acknowledgements

This work was supported by a research grants from center of excellence of medicinal chemistry, Tehran University of Medical Sciences. We thank, Ms. Shoukofeh Hassani (Lab Supervisor) for allowing us to use their lab facilities.

References

[1] G.J. Peters, H.H. Backus, S. Freemantle, B. van Triest, G. Codacci-Pisanelli, C.L. van der Wilt, K. Smid, J. Lunec, A.H. Calvert, S. Marsh, H.L. McLeod, E. Bloemena, S. Meijer, G. Jansen, C.J. van Groeningen, H.M. Pinedo, Induction of thymidylate synthase as a 5-fluorouracil resistance mechanism, Biochim. Biophys. Acta 1587 (2002) 194–205.
[2] K.H. Elstein, M.L. Mole, R.W. Setzer, R.M. Zucker, R.J. Kavlock, J.M. Rogers, C. Lau, Nucleoside-mediated mitigation of 5-fluorouracil-induced toxicity in synchronized murine erythroleukemic cells, Toxicol. Appl. Pharmacol. 146 (1997) 29–39.
[3] K. Ghoshal, S.T. Jacob, An alternative molecular mechanism of action of 5-fluorouracil, a potent anticancer drug, Biochem. Pharmacol. 53 (1997) 1569–1575.
[4] E. Ojima, Y. Inoue, H. Watanabe, J. Hiro, Y. Toiyama, C. Miki, M. Kusunoki, The optimal schedule for 5-fluorouracil radiosensitization in colon cancer cell lines, Oncol. Rep. 16 (2006) 1085–1091.
[5] M. Malet-Martino, R. Martino, Clinical studies of three oral prodrugs of 5-fluorouracil (capecitabine, UFT, S-1): a review, Oncologist 7 (2002) 288–323.
[6] J.E. Biaglow, M.E. Varnes, L. Roizen-Towle, E.P. Clark, E.R. Epp, M.B. Astor, E.J. Hall, Biochemistry of reduction of nitro heterocycles, Biochem. Pharmacol. 35 (1986) 77–90.
[7] P. Mason, J.L. Holtzman, The role of catalytic superoxide formation in the O_2 inhibition of nitroreductase, Biochem. Biophys. Res. Commun. 67 (1975) 1267–1275.
[8] P. Wardman, Eric. D-Clarke, Oxygen inhibition of nitroreductase: electron transfer from nitro radical-anions to oxygen, Biochem. Biophys. Res. Commun. 69 (1976) 942–949.
[9] P. Wardman, Some reactions and properties of nitro radical-anions important in biology and medicine, Environ. Health Perspect. 64 (1985) 309–320.
[10] A. Khalaj, A.R. Doroudi, S.N. Ostad, M.R. Khoshayand, M. Babai, N. Adibpour, Synthesis, aerobic cytotoxicity, and radiosensitizing activity of novel 2,4-dinitrophenylamine tethered 5-fluorouracil and hydroxyurea, Bioorg. Med. Chem. Lett. 16 (2006) 6034–6038.
[11] B.D. Palmer, W.R. Wilson, S.M. Pullen, W.A. Denny, Hypoxia-selective antitumor agents. 3. Relationships between structure and cytotoxicity against cultured tumor cells for substituted N, N-bis(2-chloroethyl)anilines, J. Med. Chem. 33 (1990) 112–121.
[12] B.D. Palmer, W.R. Wilson, S. Cliff, W.A. Denny, Hypoxia-selective antitumor agents. 5. Synthesis of water-soluble nitroaniline mustards with selective cytotoxicity for hypoxic mammalian cells, J. Med. Chem. 35 (1992) 3214–3222.
[13] D.F. Lewis, Molecular orbital calculations on tumour-inhibitory aniline mustards: QSARs, Xenobiotica 19 (1989) 243–251.
[14] P.G. Gill, J.W. Denham, G.G. Jamieson, P.G. Devitt, E. Yeoh, C. Olweny, Patterns of treatment failure and prognostic factors associated with the treatment of esophageal carcinoma with chemotherapy and radiotherapy either as sole treatment or followed by surgery, J. Clin. Oncol. 10 (1992) 1037–1043.
[15] D.C. Carter, J.X. Ho, Structure of serum albumin, Adv. Prot. Chem. 45 (1994) 153–203.
[16] T. Peters, All about Albumin: Biochemistry, Genetics, and Medical Applications, Academic Press, Berlin, 1996.
[17] X.M. He, D.C. Carter, Atomic structure and chemistry of human serum albumin, Nature 358 (1992) 209–215.
[18] S. Hamdani, D. Joly, R. Carpentier, H.A. Tajmir-Riahi, The effect of methylamine on the solution structures of human and bovine serum albumins, J. Mol. Struct. 936 (2009) 80–86.
[19] P.N. Naik, S.A. Chimatadar, S.T. Nandibewoor, Interaction between a potent corticosteroid drug – dexamethasone with bovine serum albumin and human serum albumin: a fluorescence quenching and fourier transformation infrared spectroscopy study, J. Photochem. Photobiol. B 100 (2010) 147–159.
[20] S. Dubeau, P. Bourassa, T.J. Thomas, H.A. Tajmir-Riahi, Biogenic and synthetic polyamines bind bovine serum albumin, Biomacromolecules 11 (2010) 1507–1515.
[21] L. Painter, M.M. Harding, P.J. Beeby, Synthesis and interaction with human serum albumin of the first 3, 18-disubstituted derivative of bilirubin, J. Chem. Soc., Perkin Trans. 1 (1998) 3041–3044.
[22] S.Y. Lin, M.J. Li, Y.S. Wei, Ethanol or/and captopril-induced precipitation and secondary conformational changes of human serum albumin, Spectrochim. Acta A, Mol. Biomol. Spectrosc. 60 (2004) 3107–3111.
[23] F. Dousseau, M. Therrien, M. Pézolet, On the spectral subtraction of water from the FT-IR spectra of aqueous solutions of proteins, Appl. Spectrosc. 43 (1989) 538–542.
[24] D.M. Byler, H. Susi, Examination of the secondary structure of proteins by deconvolved FTIR spectra, Biopolymers 25 (1986) 469–487.
[25] R. Beauchemin, C.N. N'Soukpoe-Kossi, T.J. Thomas, T. Thomas, R. Carpentier, H.A. Tajmir-Riahi, Polyamine analogues bind human serum albumin, Biomacromolecules 8 (2007) 3177–3183.
[26] A. Ahmed-Ouameur, H.A. Tajmir-Riahi, R. Carpentier, A quantitative secondary structure analysis of the 33 kDa extrinsic polypeptide of photosystem II by FTIR spectroscopy, FEBS Lett. 363 (1995) 65–68.
[27] K. Connors, Binding Constants: The measurement of Molecular Complex Stability, John Wiley & Sons, New York, 1987.
[28] K. Arnold, L. Bordoli, J. Kopp, T. Schwede, The SWISS-MODEL workspace: a web-based environment for protein structure homology modelling, Bioinformatics 22 (2006) 195–201.
[29] B. Rost, Twilight zone of protein sequence alignments, Prot. Eng. 12 (1999) 85–94.
[30] S. Sugio, A. Kashima, S. Mochizuki, M. Noda, K. Kobayashi, Crystal structure of human serum albumin at 2.5 A resolution, Prot. Eng. 12 (1999) 439–446.
[31] T. Schwede, J. Kopp, N. Guex, M.C. Peitsch, SWISS-MODEL: an automated protein homology-modeling server, Nucl. Acids. Res. 31 (2003) 3381–3385.
[32] F.J. Solis, R.J.-B. Wets, Minimization by random search techniques, Math. Oper. Res. 6 (1981) 19–30.
[33] H.I. Ali, T. Fujita, E. Akaho, T. Nagamatsu, A comparative study of AutoDock and PMF scoring performances, and SAR of 2-substituted pyrazolotriazolo-pyrimidines and 4-substituted pyrazolopyrimidines as potent xanthine oxidase inhibitors, J. Comput. Aid. Mol. Des. 24 (2010) 57–75.
[34] S. Krimm, J. Bandekar, Vibrational spectroscopy and conformation of peptides, polypeptides, and proteins, Adv. Prot. Chem. 38 (1986) 181–364.
[35] A. Ahmed-Ouameur, S. Diamantoglou, M.R. Sedaghat-Herati, S. Nafisi, R. Carpentier, H.A. Tajmir-Riahi, The effects of drug complexation on the stability and conformation of human serum albumin: protein unfolding, Cell Biochem. Biophys. 45 (2006) 203–214.
[36] P. Bourassa, C.D. Kanakis, P. Tarantilis, M.G. Pollissiou, H.A. Tajmir-Riahi, Resveratrol, genistein, and curcumin bind bovine serum albumin (dagger), J. Phys. Chem. B 114 (2010) 3348–3354.
[37] J. Tian, J. Liu, Z. Hu, X. Chen, Interaction of wogonin with bovine serum albumin, Bioorg. Med. Chem. 13 (2005) 4124–4129.
[38] J. Grdadolnik, Saturation effects in FTIR spectroscopy: intensity of amide I and amide II bands in protein spectra, Acta Chim. Slov. 50 (2003) 777–788.
[39] P. Bourassa, S. Dubeau, G.M. Maharvi, A.H. Fauq, T.J. Thomas, H.A. Tajmir-Riahi, Locating the binding sites of anticancer tamoxifen and its metabolites 4-hydroxytamoxifen and endoxifen on bovine serum albumin, Eur. J. Med. Chem. 46 (2011) 4344–4353.
[40] J. Liu, J. Tian, Z. Hu, Binding of isofraxidin to bovine serum albumin, Biopolymers 73 (2004) 443–450.
[41] U. Kragh-Hansen, Structure and ligand binding properties of human serum albumin, Dan. Med. Bull. 37 (1990) 57–84.